SEDIMENTOLOGY the journal of the International Association of Sedimentologists

Sedimentology (2009) **56,** 1275–1291 doi: 10.1111/j.1365-3091.2008.01033.x

Stromatolites in the Late Ordovician Eureka Quartzite: implications for microbial growth and preservation in siliciclastic settings

PETER A. DRUSCHKE*, GANQING JIANG*, THOMAS B. ANDERSON† and ANDREW D. HANSON*

**Department of Geoscience, University of Nevada, Las Vegas, NV 89154-4010, USA (E-mail: druschke@unlv.nevada.edu; ganqing.Jiang@unlv.edu)*

†Department of Geology, Sonoma State University, Rohnert Park, CA 94928, USA

Associate Editor – Daniel Ariztegui

ABSTRACT

Well-preserved siliciclastic domal stromatolites, up to 2 m wide and 1·5 m high, are found in a 10 to 15 m thick interval within the Late Ordovician Eureka Quartzite of Southern Nevada and Eastern California, USA. These stromatolites appear as either isolated features or patchy clusters that contain more than 70% by volume quartz grains; their association with planar, trough and herringbone cross-bedding suggests that they were formed in an upper shoreface environment with high hydraulic energy. In this environment, sand bars or dunes may have provided localized shelter for initial microbial mat colonization. Biostabilization and early lithification of microbial mats effectively prevented erosion during tidal flushing and storm surges, and the prevalence of translucent quartz sand grains permitted light penetration into the sediment, leading to thick microbial mat accretion and the formation of domal stromatolites. Decimetre-scale to metre-scale stromatolite domes may have served as localized shelter and nucleation sites for further microbial mat colonization, forming patchy stromatolite clusters. Enrichment of iron minerals, including pyrite and hematite, within dark internal laminae of the stromatolites indicates anaerobic mineralization of microbial mats. The occurrence of stromatolites in the Eureka Quartzite provides an example of microbial growth in highly stressed, siliciclastic sedimentary environments, in which microbial communities may have been able to create microenvironments promoting early cementation/lithification essential for the growth and preservation of siliciclastic stromatolites.

Keywords Eureka Quartzite, Late Ordovician, microbial mats, siliciclastic stromatolite, Western Laurentia.

INTRODUCTION

In modern shallow marine environments, microbial mats are common on both siliciclastic and carbonate substrates (Gerdes *et al.*, 2000; Riding, 2000; Porada & Bouougri, 2007) but siliciclastic stromatolites are scarce compared to their carbonate counterparts in the rock record. The paucity of stromatolites in siliciclastic strata may relate to physical conditions and processes within the depositional environment that inhibit stromatolite growth and preservation. For example, due to the generally high sediment mobility in siliciclastic environments, frequent disturbance by waves or tides may prevent the development of thick microbial mats unless episodes of low or zero sedimentation occur to allow microbial communities sufficient time to repeatedly re-establish and stabilize on sediment surfaces (Reineck & Gerdes, 1997; Lee *et al.*, 2000; Draganits & Noffke,

2004). In siliciclastic environments with a turbid water column, stromatolite growth may be inhibited by reduced light penetration. Environments with mixed grain-sizes and composition may not be as favourable for microbial mat growth as those with predominately clean, fine-grained to medium-grained quartz sand (Gerdes & Krumbein, 1987; Noffke *et al.*, 2001, 2002).

These environmental limitations, however, are not unique to siliciclastic settings. Abundant, well-preserved stromatolites have been documented in carbonate environments with comparable sediment grain-size, water depth, wave energy and nutrient supply. A more fundamental control on the growth and preservation of siliciclastic stromatolites may be early cementation/lithification (Grotzinger & Knoll, 1999). Trapping and binding of sediment particles by microbial mats is a phenomenon common in both siliciclastic and carbonate environments but these processes alone are insufficient to permanently stabilize sediment in the absence of early cementation (Grotzinger & Knoll, 1999; Pratt, 1979). Under the appropriate conditions (e.g. a high Ca^{2+}/CO_3^{2-} ratio), early lithification of microbial mats may be induced by cyanobacterial sheath calcification during photosynthesis (Riding, 2006; Arp *et al.*, 2001; Kah & Riding, 2007). However, microbial mat degradation and heterotrophic bacterial metabolism may play a more critical role (Pratt, 1984, 2001; Chafetz & Buczynski, 1992; Knoll & Semikhatov, 1998; Bartley *et al.*, 2000). In the latter lithification process, carbonate substrates are more favourable for catalyzing mineral overgrowth over pre-existing carbonate crystals. In siliciclastic environments, stromatolites may experience early lithification only when localized environments induce high carbonate alkalinity through evaporation (Braga & Martín, 2000) or by strong mineralization of microbial mats.

This paper reports well-preserved stromatolites from the Late Ordovician Eureka Quartzite in Southern Nevada and South-eastern California of the Western USA (Fig. 1A). The Eureka Quartzite in this region consists predominantly of fine-grained to medium-grained quartz arenite deposited in tropical, high-energy shallow marine environments. The presence of centimetre-scale to metre-scale stromatolites in such a high-energy

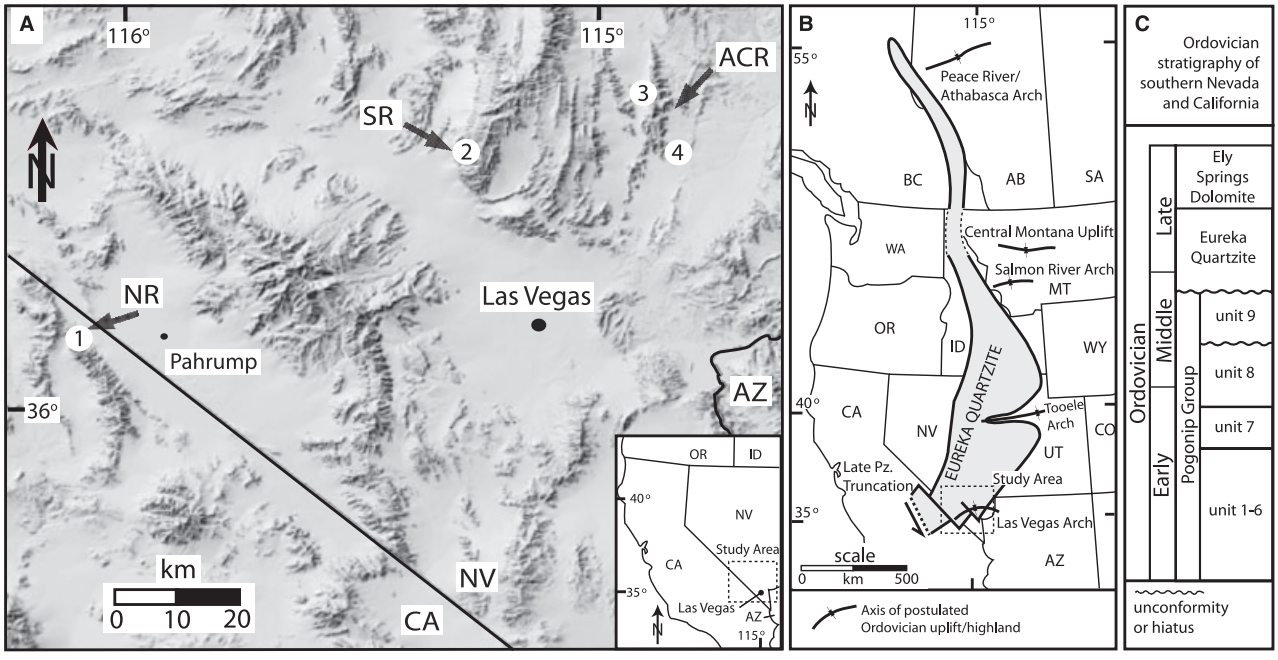

Fig. 1. (A) Location of measured sections in South-eastern California and Southern Nevada in the vicinity of Las Vegas: 1: Northern Nopah Range (NR); 2: Southern Sheep Range (SR); 3: North-western Arrow Canyon Range (ACR); 4: Silica Quarry within the South-eastern Arrow Canyon Range. (B) Generalized map showing the distribution of the Eureka Quartzite and its equivalent units along the western margin of Laurentia. Dashed boundaries indicate where original continuity is inferred (modified from Ketner, 1968). The 'Las Vegas Arch' (Cooper & Keller, 2001) refers to a potential Ordovician highland that may have influenced the distribution and thickness of the Eureka Quartzite. Additional 'arch' locations are from Burchfiel *et al.* (1992). (C) Generalized Ordovician stratigraphy of California and Nevada (modified from Cooper & Keller, 2001).

shallow marine setting provides insight into the ability of benthonic microbial mats to: (i) colonize highly stressed siliciclastic depositional environments; and (ii) create localized chemical conditions through mat mineralization that possibly facilitate early lithification and, ultimately, stromatolite preservation.

GEOLOGICAL SETTING

The Ordovician Eureka Quartzite represents the only significant sandstone interval within the several kilometres thick Middle Cambrian to Devonian carbonate succession of the Western USA. The Eureka Quartzite is composed predominantly of fine-grained to medium-grained, silica-cemented quartz arenite (Ketner, 1968). The term 'quartzite' is a relic of antiquated sandstone classification terminology but, nevertheless, survives as part of the formal stratigraphic nomenclature of the Eureka Quartzite.

Tectonic framework

The Eureka Quartzite was deposited on a west-dipping carbonate ramp along the Western Laurentian margin during Middle to Late Ordovician times. The Western Laurentian margin has generally been considered as a passive margin from the latest Neoproterozoic to Late Devonian (Burchfiel *et al.*, 1992; Poole *et al.*, 1992). The Eureka Quartzite and correlative units crop out over a vast area of >450 000 km^2 in Western North America, including portions of Eastern California, Nevada, Western Utah, Southern Idaho and extend as far north as the Athabasca-Peace River Arch in Alberta/British Columbia, Canada (Ketner, 1968; Gehrels *et al.*, 1995; Fig. 1B). The thickness of the Eureka Quartzite and its equivalents vary regionally, from a maximum of 400 to 520 m in the Peace River Arch of Canada and Northern Nevada to an average of *ca* 40 m in Southern Nevada and Eastern California (Ketner, 1968).

One puzzling point related to the deposition of the Eureka Quartzite is the source of the enormous volume of quartz sand (> 50 000 km^3; Ketner, 1968; Gehrels *et al.*, 1995) on a carbonate platform. Ketner (1968) interpreted that recycled Cambrian quartzites of the Peace River Arch in North-western Canada are the primary source of the Eureka Quartzite, transported margin-wide via longshore drift. Evidence supporting this interpretation includes an overall southward thinning, fining and maturing trend of quartz arenite units along the Western Laurentian margin (Ketner, 1968) and the presence of 1·8 to 2·4 Ga detrital zircons within the Eureka Quartzite, which is consistent with the age distribution of Cambrian quartz arenites in the Peace River Arch (Gehrels *et al.*, 1995).

The sections measured during this investigation are located in Southern Nevada and South-eastern California (Fig. 1A). This region represents the southern limit of the Eureka Quartzite in the Western USA, as the early Palaeozoic platform was truncated by late Palaeozoic sinistral strike-slip faulting that translated earlier platform deposits south-eastward to Sonora, Mexico (Ketner, 1986; Stone & Stevens, 1988). The original continuity of the lower Palaeozoic platform has been disrupted further by the Cretaceous Sevier orogeny and Cenozoic extensional faults along much of the North American Cordillera (Poole *et al.*, 1992). Nonetheless, well-preserved Cambrian to Ordovician successions are exposed in this region and the Eureka Quartzite is a prominent marker for stratigraphic correlation in the field.

Stratigraphy and age

In Southern Nevada and Eastern California, the Eureka Quartzite rests on the Middle Ordovician Pogonip Group and is overlain by the Late Ordovician Ely Springs Dolomite (Fig. 1C). The upper boundary of the Eureka Quartzite is conformable but the lower boundary is marked by a major karstic unconformity with considerable erosion (Cooper & Keller, 2001).

The age of the Eureka Quartzite is roughly constrained by the biostratigraphy and chemostratigraphy of underlying and overlying carbonate formations in Central Nevada. The *Phragmodus undatus–Plectodina tenuis* conodont zones of the upper Copenhagen Formation (Harris *et al.*, 1979) below the Eureka Quartzite are associated with a prominent positive $\delta^{13}C$ excursion up to +3·7‰ (Saltzman & Young, 2005), which has been correlated with the conodont zones and a $\delta^{13}C$ peak of late Chatfieldian Stage (middle Mohawkian) in Eastern Laurentia (Patzkowsky *et al.*, 1997; Ludvigson *et al.*, 2004). The basal Hanson Creek Formation (equivalent to the Ely Springs Dolomite in Fig. 1C) contains conodonts of late Edenian (early Cincinnatian) age (Sweet, 2000). Altogether, the depositional age of the Eureka Quartzite may range from late Chatfieldian (middle Mohawkian) to late Edenian Stage (early Cincinnatian), although deposition of the lower Eureka Quartzite may have been

significantly diachronous in Southern Nevada and Eastern California.

Depositional environments

The Eureka Quartzite has generally been interpreted as shallow marine deposits based on the presence of dolostone beds, brachiopod fragments and marine trace fossils such as *Skolithos* (Ketner, 1968). Interbeds of planar and herringbone cross-bedded and bioturbated sandstone have been interpreted as deposits in shoreface environments (Miller, 1977) or tidal-influenced sand shoals, tidal flats and channels (Klein, 1975). Based on measured sections in Southern Nevada and Eastern California, five facies associations within the Eureka Quartzite are identified (FA-1 to FA-5, Fig. 2). Among these, FA-1 and FA-2 are interpreted as having deposited from a wave-dominated shoreface (Fig. 3A), while FA-4 and FA-5 formed within a wave-dominated barrier-island system (Fig. 3B). Facies Association 3

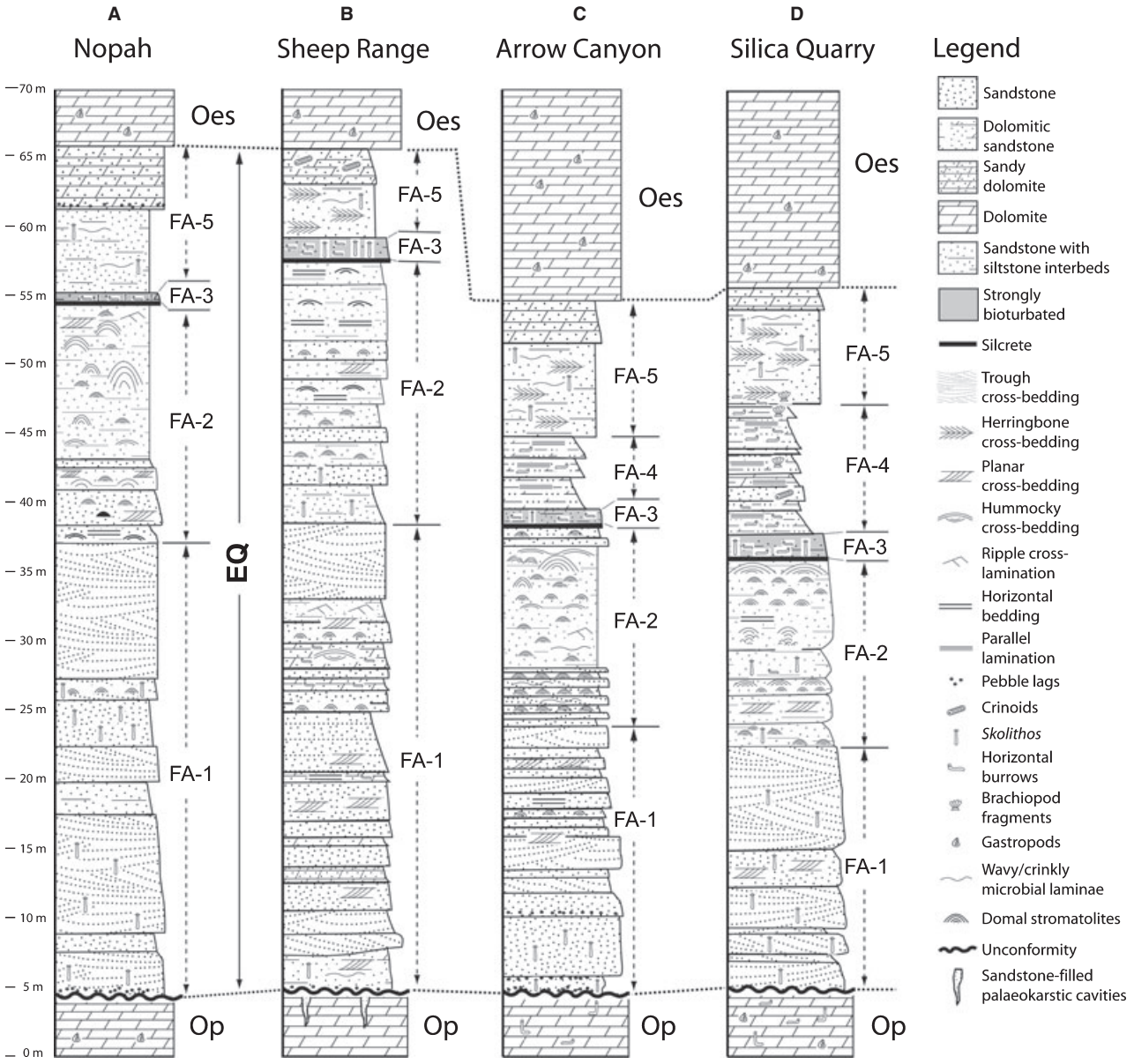

Fig. 2. Lithostratigraphic sections of the Eureka Quartzite in (A) Nopah Range, (B) Sheep Range, (C) Northern Arrow Canyon Range and (D) Silica Quarry of South-eastern Arrow Canyon Range. FA-1 to FA-5 indicate the facies associations described in the text. Domal stromatolites are found mainly in FA-2, with an up-section increase in size and abundance. Well-preserved microbial laminae and centimetre-scale columnar stromatolites are present in FA-5, especially in the northern Arrow Canyon and Silica Quarry sections. Op, Pogonip; Oes, Ely Springs Dolomite; EQ, Eureka Quartzite.

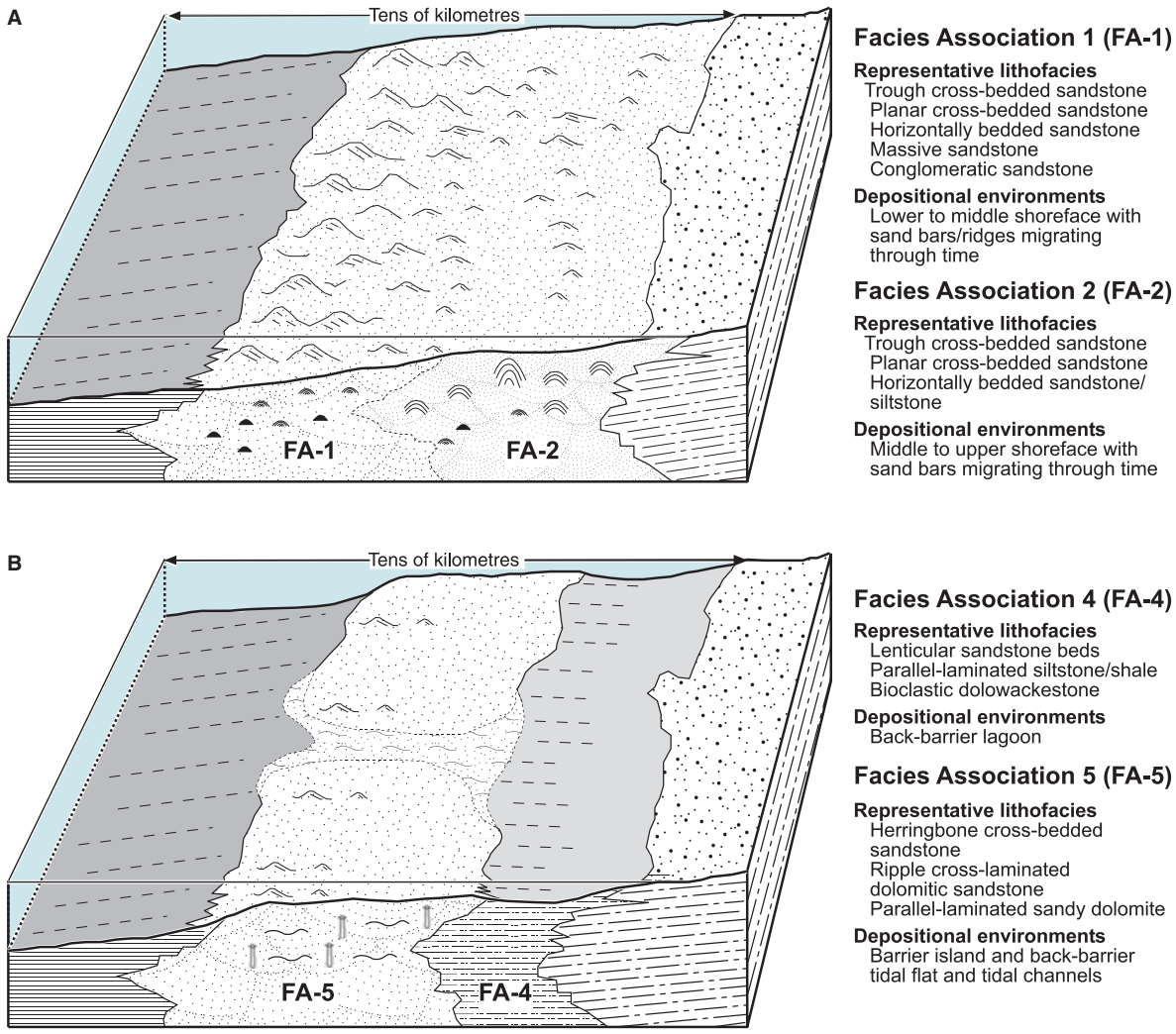

Fig. 3. Palaeoenvironmental interpretation for the facies associations of the Eureka Quartzite (Fig. 4). (A) FA-1 and FA-2 are interpreted as having been deposited in a wave-dominated shoreface where FA-1 may record middle to lower shoreface facies and FA-2 records middle to upper shoreface facies. (B) FA-4 and FA-5 are interpreted as deposited in a wave-dominated and tidal-influenced barrier-island system where FA-4 represents lagoonal deposits and FA-5 represents back-barrier tidal flat deposits.

marks a regionally persistent hardground above an exposure surface formed during transgression.

Facies Association 1 consists of cross-bedded, fine-grained to medium-grained quartz arenite and comprises the lower portions of the four measured sections. Lithofacies include planar cross-bedded sandstone (Fig. 4A), trough cross-bedded sandstone (Fig. 4B), horizontally bedded sandstone and massive sandstone beds. At the basal Eureka Quartzite, conglomeratic sandstone containing chert pebbles and brachiopod fragments is present as lag deposits along bedding planes. The trace fossil *Skolithos* is common, giving outcrops a pock-marked appearance. Facies Association 1 is interpreted as deposits from lower to middle shoreface environments where moderate to low-angle planar cross-stratification was formed near the centre of sand bars or sand ridges and trough cross-stratification was formed at their margins or within tidal channels (Tillman & Martinsen, 1984; Gaynor & Swift, 1988). Horizontally bedded sandstone may have formed in interbar areas, with massive beds accumulating during storm episodes (Martini *et al.*, 1995). Only small domal stromatolites with <10 cm synoptic relief and their fragments were observed within FA-1.

Facies Association 2 comprises fine-grained to medium-grained quartz arenite with subordinate siltstone interbeds. Major lithofacies include planar cross-bedded sandstone, trough cross-bedded sandstone, horizontally bedded sandstone/siltstone and, less commonly, ripple cross-laminated

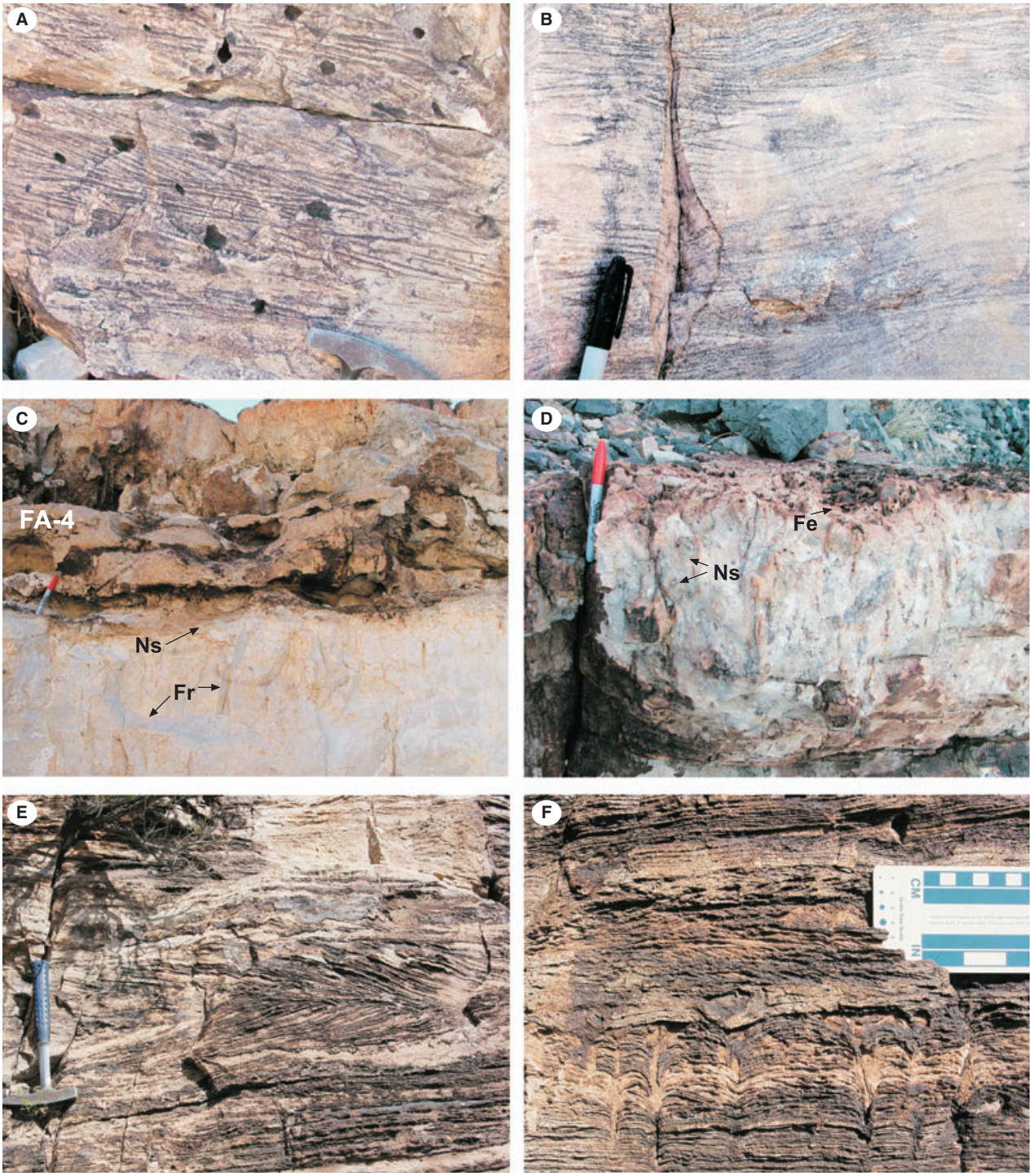

Fig. 4. Sedimentary structures of the Eureka Quartzite. (A) Low-angle planar cross-bedding from FA-1 of the Silica Quarry section (Fig. 2D). (B) Low-angle trough cross-bedding from the northern Arrow Canyon Range section (Fig. 2C). (C) FA-3 from the Silica Quarry section. In this section, FA-3 is composed of a 1·5 m thick, highly bioturbated fine-grained quartz sandstone and siltstone above a 15 cm thick horizon that contains nodular silica (Ns) and desiccation cracks (Fr). (D) Interpreted exposure surface below FA-3 in the northern Arrow Canyon section (Fig. 2C) containing iron oxides (Fe) and Ns. (E) Herringbone cross-stratification of FA-5 from the northern Arrow Canyon Range section (Fig. 2C). (F) Microbial laminae, vertical burrows (lower portion of image) and ripple cross-lamination of FA-5 from the northern Arrow Canyon Range section (Fig. 2C). Hammer head used for scale in panels (A) and (E) is 18 cm long. Pens used for scale in panels (B) to (D) are 13 cm long with a 5 cm cap.

siltstone. Compared with FA-1, FA-2 contains relatively more fine-grained sandstone and siltstone beds but less-abundant trough cross-stratification. It is interpreted as having formed in middle to upper shoreface environments with less prominent sand bars or ridges. Large sand bars or ridges within FA-1 may have provided a sheltered setting for the proximal shoreface of FA-2, but wave activity was not sufficiently blocked to form a true barrier and back-barrier lagoon system. The majority of the domal stromatolites reported in this paper are from FA-2.

Facies Association 3 consists of a 0·5 to 1·5 m thick interval characterized by intensely bioturbated, fine-grained quartz sandstone and siltstone. The basal interval of FA-3 contains a 5 to 30 cm thick horizon enriched in iron oxides and nodular silica that in some cases contains desiccation cracks (Fig. 4C and D). Facies Association 3 thus is interpreted as a regionally persistent, condensed hardground formed along the transgressive surface after exposure of the lower Eureka Quartzite shoreface environments.

Facies Association 4 is present only in the Arrow Canyon sections (Fig. 2C and D) and consists of parallel-laminated siltstone/shale, lenticular fine-grained sandstone and bioclastic dolowackestone. Abundant trace fossils including *Chondrites* and *Planolites* (Miller, 1977) are present. Additional fossils in this facies include partially disarticulated crinoid stalks and brachiopod fragments. No stromatolites or microbial laminae are observed in FA-4. The localized, dominantly fine-grained deposits of FA-4 are interpreted as low-energy deposits formed in a back-barrier lagoon.

Facies Association 5 is composed of herringbone cross-bedded quartz arenite (Fig. 4E), ripple cross-laminated dolomitic quartz arenite and parallel-laminated sandy dolomite. In the Arrow Canyon Range (localities 3 and 4, Fig. 1), well-preserved flat and wavy microbial laminae are found in association with abundant vertical burrows (Fig. 4F). These facies are interpreted as deposits from a back-barrier tidal flat where herringbone cross-stratification probably formed within tidal channels (Fig. 3B).

SILICICLASTIC MICROBIAL STRUCTURES

Microbial structures including domal stromatolites and bioturbated microbial laminae are present in all measured sections within the study area. Well-preserved domal stromatolites occur mainly in the upper Eureka Quartzite (FA-2), although smaller and less well-preserved examples also appear sporadically in the lower part (FA-1). Bioturbated microbial laminae are best-exposed within the uppermost Eureka Quartzite (FA-5). All occurrences are associated with cross-bedded sandstones that volumetrically contain >70% framework quartz grains, indicating high-energy conditions.

Domal stromatolites

Stratigraphic occurrences and morphological features

The best-preserved domal stromatolites occur in the Arrow Canyon Range. Within a 15 m thick interval (FA-2 in Fig. 2C and D), stromatolite domes increase in size and abundance up-section. In the lower part of FA-2, crinkled microbial laminae grade upward into centimetre-scale, dark-grey to brownish asymmetric domes with 5 to 10 cm synoptic relief (Fig. 5A and B). These small domes are laterally discontinuous but widespread along traceable horizons. Inter-dome areas are filled with white-coloured, medium-grained quartz arenite that occasionally displays low-angle planar cross-stratification. Up-section, small domes grade into larger and more conspicuous stromatolite domes commonly 30 to 50 cm wide and 30 to 80 cm high (Fig. 5C); a few occurrences are even larger, up to 2 m wide and 1·5 m high. Large domes commonly appear as isolated features with steep (> 45°) flanks in contact with trough cross-bedded or horizontally bedded quartz arenite. The uppermost 3 m of the stromatolite succession is characterized by large, regularly distributed, laterally linked hemispheroids (LLH; Fig. 5D), which are similar to LLH domes described from carbonate depositional environments (Logan *et al.*, 1964). In the Silica Quarry section (Fig. 2D), the middle part of the stromatolite succession also contains stromatolite clusters, with larger stromatolite domes superimposed over a series of smaller domal forms (Fig. 5E and F). These clusters are either oriented vertically (Fig. 5F) or display 15 to 20° of inclination with respect to overlying bedding (Fig. 5E).

In FA-2 of the Nopah Range section (Fig. 2A), a similar stromatolite-bearing interval occurs, with centimetre-scale domal stromatolites at the base of FA-2 and more abundant and larger domes up-section. Less abundant and less well-preserved stromatolites are also present in the Sheep Range section (Fig. 2B). Here isolated, centimetre-scale

Fig. 5. Domal stromatolites from FA-2 of the Eureka Quartzite. (A) Dark grey to brownish stromatolite domes. (B) An isolated stromatolite dome. (C) An isolated stromatolite dome with steep margins. (D) Laterally linked stromatolite domes. All examples are from FA-2 of the northern Arrow Canyon section (Fig. 2C). (E) Stromatolite clusters with 15° angle inclined to overlying and underlying strata. (F) Stromatolite clusters vertical to overlying bedding. Both (E) and (F) are from FA-2 of the Silica Quarry section (Fig. 2D). Hammer used for scale in panels (A) to (E) is 32 cm long and the head is 18 cm wide. Pen used for scale in panel (F) is 13 cm long with a 5 cm cap.

domal stromatolites are found to be associated with low angle, planar cross-bedded or horizontally bedded quartz sandstone.

In addition to the more common occurrence in FA-2, small domal stromatolites with dimensions of 5 to 15 cm wide and 3 to 8 cm high are also

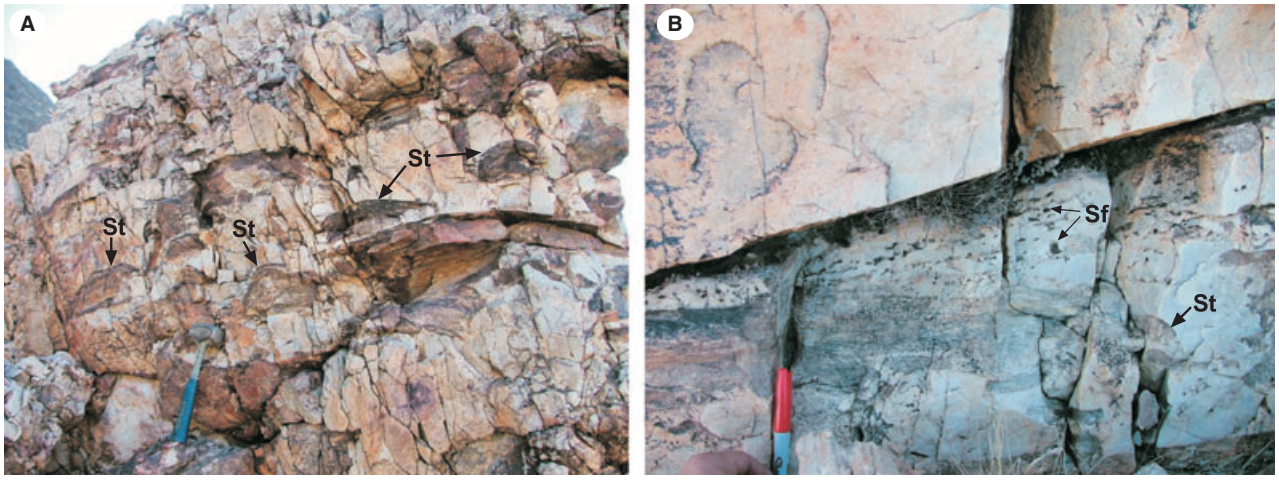

Fig. 6. Stromatolites from FA-1 of the Eureka Quartzite. (A) Stromatolite domes (St) with dimensions of 5 to 15 cm wide and 3 to 8 cm high from FA-1 of the Nopah Range section (Fig. 2A). Hammer for scale is 32 cm long. (B) St and reworked stromatolite fragments (Sf) along bedding planes of low-angle planar cross-beds. From FA-1 of the northern Arrow Canyon section (Fig. 2C). Pen for scale is 13 cm long with a 5 cm cap.

observed in FA-1. These stromatolites are brownish to grey in colour, in contrast to the hosting white quartz arenite, and appear either as isolated forms or, in some cases, as clusters of centimetre-scale domes in planar cross-bedded quartz arenite (Fig. 6A). Broken stromatolite fragments also appear as redeposited clasts along the bedding planes of cross-beds (Fig. 6B).

Internal laminae and textures

Domal stromatolites typically contain internal laminae 1 to 5 mm thick (Fig. 7A and B). Laminae bend accordingly at the margins of the domes, with high dip angles commonly >45° and up to 80° at their steepest (Fig. 5C). Internal lamination is composed of alternating white and dark-grey layers (Fig. 7A and B) that are thicker along the growth axis. Darker layers are commonly enriched in opaque minerals (Fig. 7A and B) consisting mainly of pyrite and ferric iron oxide (hematite and/or goethite). Dark layers also contain clay minerals (kaolinite), silt-sized quartz grains and subordinate mica and dolomite cements in interstitial spaces (Fig. 7C to F). Both white and dark layers are grain-supported with moderately to well-rounded quartz grains but, in most cases, the dark layers are slightly enriched in finer grain-sizes and thus relatively less well-sorted (Fig. 7C and D).

The internal laminae of some domal stromatolites are amalgamated. In these examples only the thicker dark laminae show the morphological shape of the stromatolites (Fig. 8A). These visible laminae are commonly less well-sorted and finer-grained compared to their underlying and overlying intervals and contain more iron minerals and kaolinite in interstitial spaces (Fig. 8B). Intervals between these visible laminae appear 'massive' and only thin, faint lamination can be seen on weathered surfaces. However, even in these 'massive' intervals, iron minerals (pyrite and hematite) and clays are present in intergranular spaces (Fig. 8C). In contrast, few clay or iron minerals are present in the white quartz arenite surrounding the stromatolites.

Interpretation

The domal structures within the Eureka Quartzite have been noted by previous workers but no detailed description has been available. Interpretations of these structures were based on a single section or a single specimen and include: (i) load structures (Miller, 1975, 1977); (ii) hummocky cross-stratification; and (iii) algal stromatolites (Langenheim & Horn, 1978). However, as described above, the lack of convex-down laminae and erosional bases, the steep flanks with dips >45° exceeding the angle of repose for unconsolidated sand (Garlick, 1988; Schieber, 1999) and the lack of laminae thickening in troughs do not favour a hummocky cross-stratification interpretation. Similarly, the lack of convex-down bedding planes or laminae and absence of flame, dish and pillar structures or convolute bedding in these domal structures do not support the load structure interpretation. In contrast, the positive morphological features, the presence of reworked microbial fragments and distinctive internal laminae enriched in iron minerals indicate their biogenic origin as siliciclastic stromatolites.

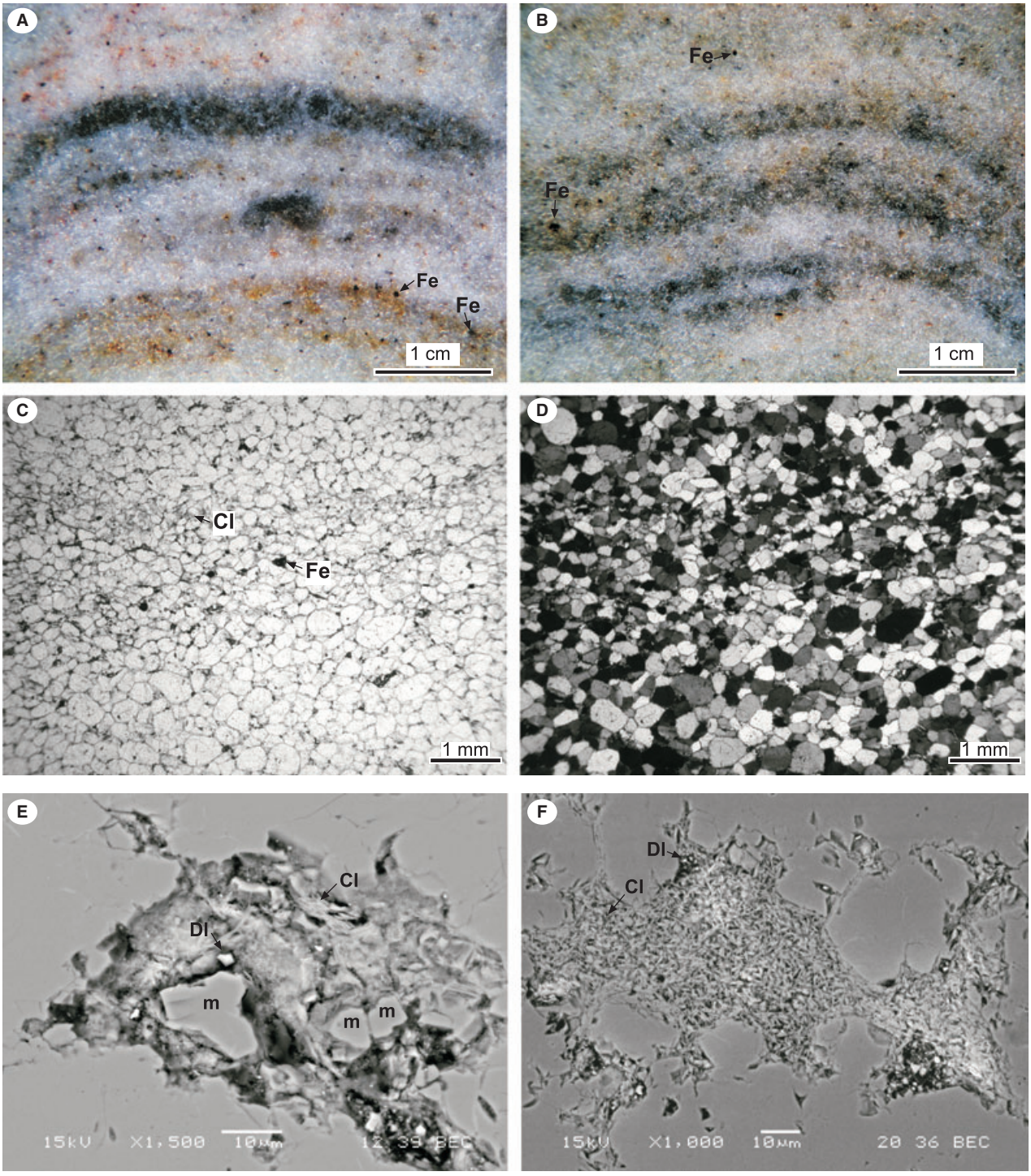

Fig. 7. Internal laminae and texture of domal stromatolites. (A) and (B) Polished thick sections showing alternating dark and light laminae. The dark laminae are enriched in iron minerals (Fe) including pyrite and hematite. (C) Photomicrograph of a dark lamina (plane-polarized light). The dark lamina is relatively finer grained, less well-sorted and more enriched in Fe and clay (Cl) compared with the light lamina. (D) Same image as (C) with crossed nichols. (E) SEM image of interstitial pores filled by quartz silt (m), Cl and microcrystalline dolomite (Dl) from the dark lamina in (C). (F) SEM image of interstitial pores filled mainly with Cl and Dl. Clay mineralogy is dominantly kaolinite, associated with minor mica.

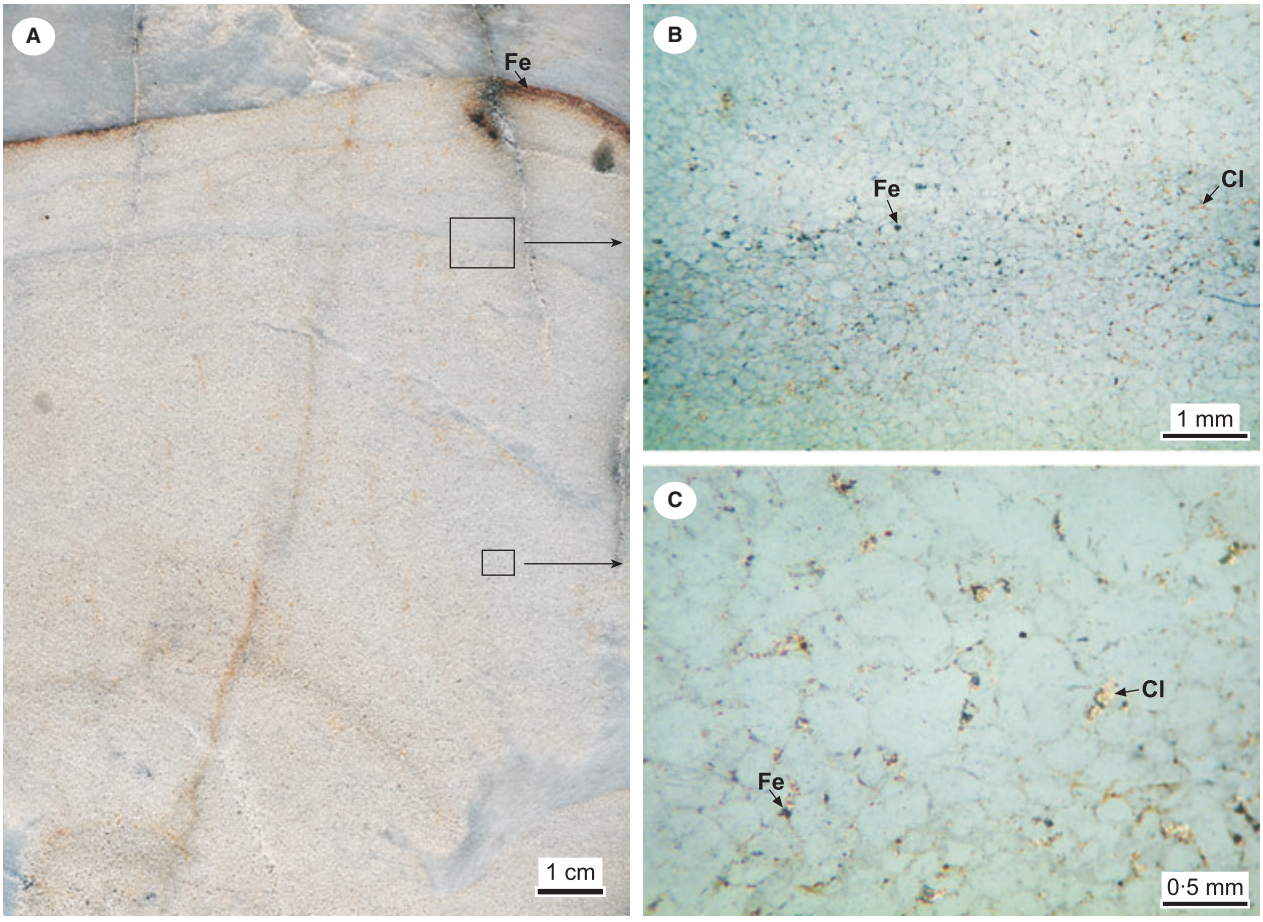

Fig. 8. (A) Polished slab of a domal stromatolite displaying amalgamated (massive) intervals and dark laminae. The visible dark laminae contain more iron minerals (Fe) and display typical stromatolite morphology. (B) Closer view of a dark lamina showing Fe and clay (Cl) in interstitial spaces (reflected light). (C) Closer view of the amalgamated (massive) interval. Presence of Fe and Cl suggests the existence of microbial activity (reflected light).

While examples of siliciclastic stromatolites are still relatively rare compared to their carbonate counterparts, a number of notable examples have been reported, including domal stromatolites in Miocene shoreface deposits of Spain (Braga *et al.*, 1995; Martín *et al.*, 1993; Braga & Martín, 2000), in Carboniferous deltaic and shoreface deposits of Algeria (Bertrand-Sarfati, 1994), in Late Ordovician peritidal deposits of Minnesota (Davis, 1968), in Late Cambrian shoreface deposits of Israel (Soudry & Weissbrod, 1995), in Mid-Proterozoic shallow marine deposits of Montana (Schieber, 1998) and, most recently, in Devonian barrier island complexes of the Lesser Himalayas, India (Draganits & Noffke, 2004). Although the domal stromatolites in the Eureka Quartzite show morphological diversity (Fig. 5), some of them (Fig. 5A, B and D) resemble examples documented from the Mid-Proterozoic Mount Shields Formation of Montana (Schieber, 1998; fig. 22), Late Ordovician New Richmond Sandstone (Davis, 1968; fig. 2), Early Devonian Muth Formation of NW Himalayas (Draganits & Noffke, 2004; figs 4 and 5) and the Miocene Sorbas Member in the Sorbas Basin of Spain (Braga & Martín, 2000; fig. 4).

The presence of iron minerals and disseminated dolomite cements suggests microbial mat mineralization. In modern environments, photosynthetic cyanobacteria may produce oxygen at the surface of microbial mats but, directly below the oxic surface layer, anaerobic bacteria degrade mat generated organic matter and may create a localized, strongly reducing environment (Gerdes *et al.*, 1985, 2000). Such a geochemical environment is favourable for the precipitation of calcium carbonate and 'anoxic' minerals such as pyrite, siderite, ankerite and ferroan dolomite (Schieber, 2007; Schieber & Riciputi, 2004). While organic matter and carbonate cements would rarely be preserved in the rock record due to silica replacement and microbial

degradation of organic matter during early burial, minerals such as pyrite, siderite (and their oxidized forms such as hematite and goethite) and ferroan dolomite can be a valuable indicator of the former presence of microbial mats (Noffke *et al.*, 2006; Schieber, 2007).

Patchy microbial mats may have colonized in protected areas behind sand dunes or sand ridges in a shoreface environment. Biostabilization and early lithification may have been strong, as indicated by the presence of detrital clay (kaolinite), silt-sized quartz grains, mica and relics of dolomite cements in stromatolite laminae. Trapping and binding of quartz grains abundant in ambient water of the shoreface environments may have facilitated the growth of thicker mat laminae (Noffke *et al.*, 1997, 2002; Gerdes *et al.*, 2000), especially at the crest of preliminary domes, leading to the development of larger domes with higher resistance to wave/tidal reworking. Storm events and/or sand dune migration during times of higher-energy conditions may have forced microbial mats to migrate and readjust to new niches, forming isolated domes.

Bioturbated microbial laminae

Description

Microbial laminae are associated closely with the domal stromatolites described in the previous section. Here the focus is on the flat and wavy microbial laminae with intense bioturbation in FA-5. Bioturbated flat and wavy microbial laminae form 10 to 15 cm thick intervals between herringbone cross-stratified or ripple cross-laminated, fine-grained quartz arenite (Figs 4F and 9). Microbial laminae are expressed as sub-millimetre scale, dark-grey, very fine-grained quartz arenite alternating with millimetre-scale white, fine-grained quartz arenite (Fig. 9). White laminae are commonly thicker and coarser grained than dark laminae. In some cases, amalgamated dark or white laminae form composite layers a few millimetres to 1 cm thick. Microbial laminae contain iron minerals (Fig. 9D) and disseminated dolomite cement, although these features are more abundant within dark laminae. Intervals of microbial laminae are laterally continuous for a few metres to tens of metres before being truncated by white-coloured, herringbone cross-bedded or ripple cross-laminated quartz arenite.

Abundant vertical to sub-vertical burrows are present within the microbially laminated intervals. Burrows are 0·2 to 0·5 cm in diameter and penetrate through microbial laminae for a few centimetres (Figs 4F and 9A to C). Smaller burrows were observed to originate within dark lamina; penetrate upward through the white lamina and terminate at the overlying dark lamina (Fig. 9C). Larger burrows penetrate multiple dark-white layers for up to 7 cm. Along burrow margins, microbial laminae bend downwards and form >45° dip angles with respect to bedding. Intervals containing bioturbated microbial laminae are typically truncated by an erosional surface below the overlying herringbone cross-stratified sandstone (Fig. 4F).

Interpretation

Microbial mats may have colonized the sandy tidal flat environments with shallow tidal channels (Fig. 4B). Dark laminae enriched in iron minerals may record times of relatively low-energy, slow sediment accumulation and thicker microbial mat colonization, whereas white laminae record times of relatively high-energy, high sediment supply and thin microbial mats (Noffke *et al.*, 2002). This observation is consistent with the small burrows that penetrate white laminae and terminate at dark laminae, suggesting that burrowing organisms attempted to escape burial during tidal flushing or storm events. Larger burrows may represent escape features formed during tidal channel erosion, as indicated by the erosional surface separating microbially laminated intervals from overlying herringbone cross-stratified sandstone. Rapid sediment collapse into the burrow causes microbial laminae to bend downward accordingly.

The association of microbial laminae and burrows indicates that microbial mats and burrowing (and potentially grazing) organisms coexisted in the same substrates. The lack of both microbial laminae and burrows in herringbone cross-stratified intervals suggests sedimentary controls on their habitats. This example lends support to the hypothesis that less-abundant stromatolites and microbial mats in the Phanerozoic rock record (compared to the Proterozoic) are due largely to sedimentary limitations rather than an evolutionary stress by grazing/burrowing organisms (Pratt, 1982).

DISCUSSION

Environmental controls on stromatolite growth in the Eureka Quartzite

The siliciclastic stromatolites and microbial laminae of the Eureka Quartzite are characterized by

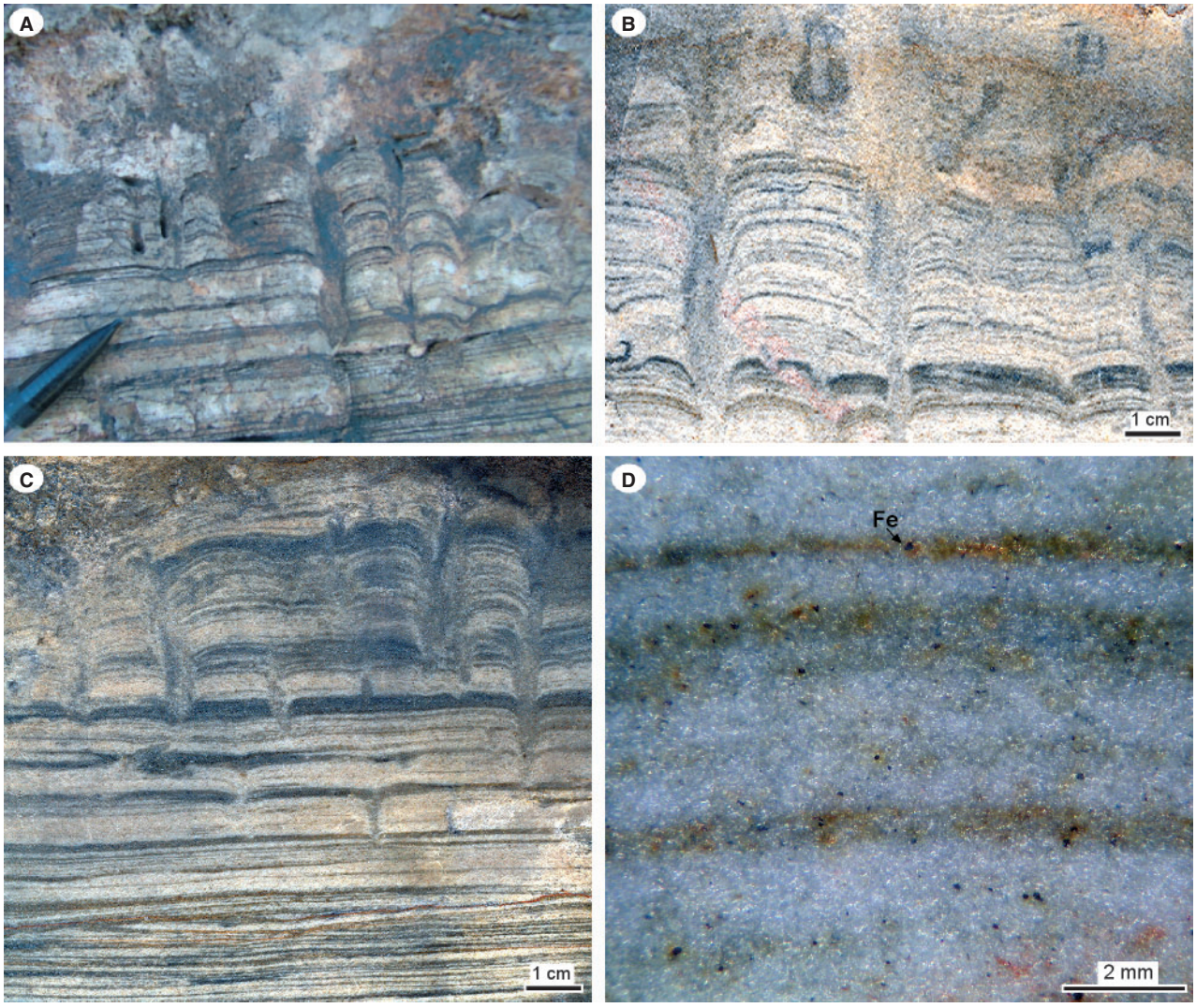

Fig. 9. (A) Microbial laminae and vertical burrows from FA-5 of the northern Arrow Canyon Range section (Fig. 2C). Burrows penetrate downward through the flat microbial laminae and both microbial laminae and burrows terminate below the overlying fine-grained quartz arenite. (B) Polished slab showing microbial laminae and burrows. Microbial laminae bend towards the burrows, suggesting that rapid escape of burrowing organisms caused slumping of sediments and subsequent bending of microbial mats. (C) Polished slab showing the association of microbial laminae and burrows. In the lower portion of the image, small burrows originate within dark lamina, penetrate upward through the white lamina and terminate at the overlying dark lamina. In the upper portion of the image, larger burrows penetrate through multiple dark and white layers, suggesting rapid escape of burrowing organisms. The burrows and microbial laminae are truncated by an erosional surface below the overlying herringbone cross-stratified, fine-grained quartz arenite. (D) Internal laminae of the siliciclastic microbial mats. Darker laminae are relatively more enriched in iron minerals (Fe).

the following features: (i) they are locally present within upper shoreface and back-barrier tidal flat environments (Fig. 3) of the upper Eureka Quartzite, where planar, trough and herringbone cross-beds formed (Fig. 4); (ii) stromatolites commonly appear as laterally discontinuous, isolated forms or patchy clusters (Fig. 5); (iii) occasionally, reworked stromatolite fragments are seen along bedding planes of cross-bed sets (Fig. 6); (iv) stromatolites and microbial laminae volumetrically consist of >70% very fine-grained to medium-grained quartz sand (Figs 7 and 8); (v) stromatolites show millimetre to sub-millimetre thick, alternating dark and light laminae (Fig. 7); and (vi) darker laminae are commonly finer-grained, less well-sorted and, preferentially, contain detrital clay, iron minerals and disseminated dolomite in interstitial spaces (Fig. 7).

These features record interactions between hydraulic action and microbial colonization.

The presence of cross-bedding in stromatolite-bearing strata indicates high-energy conditions in general, but reduction in grain-size, sorting and the presence of detrital clay in darker laminae of the stromatolites suggest that periods of relatively low-energy conditions favourable for microbial mat growth occurred. Such quiescent periods may have been of relatively short duration but were sufficient for microbial mats to re-establish. Microbes such as cyanobacteria commonly have short generation times, ranging from a few hours to a few days (Pratt, 2001). Clean, translucent, fine-grained to medium-grained quartz sand predominating in these environments may have permitted increased light penetration into the sediment and allowed filamentous cyanobacteria to grow below the sediment/water interface (Noffke *et al.*, 2002, 2003) and to repeatedly re-establish on sediment substrates following storm surges and tidal flushing. However, due to the high sediment mobility of sandy substrates, initial microbial mat colonization may have been successful only in localized areas sheltered by sand bars or dunes. Following successful colonization, biostabilization prevented the removal of microbial mats during erosion and promoted subsequent mat growth and eventual formation of large domal stromatolites. Large domes may themselves serve as localized shelter or nucleation centres for further microbial mat colonization, forming patchy stromatolite clusters.

The general lack of stromatolites and microbial laminae in the lower Eureka Quartzite (FA-1 in Figs 2 and 3) is possibly due to persistent high-energy conditions in the middle and lower shoreface environments where intensive wave erosion prevented the initial colonization of microbial mats. The sporadic presence of centimetre-scale stromatolites and reworked stromatolite fragments in FA-1 (Fig. 6) indicate that microbial colonization succeeded to some degree but failed to develop into larger forms due to high hydraulic stress. In contrast, the lack of stromatolites and microbial laminae in lagoonal environments (FA-4 in Figs 2 and 3) may be due to persistently low-energy conditions in which suspended mud and silt may have shielded potential photosynthetic mat builders from sunlight. Both modern and ancient analogues suggest that microbial mats may preferentially develop in moderate hydrodynamic conditions where waves or tides prevent the deposition of mud but lack the energy required to remove bacterially bound sand grains under fair-weather conditions (Schwartz *et al.*, 1975; Gerdes *et al.*, 2000; Noffke *et al.*, 2001, 2002).

Stromatolite preservation in the Eureka Quartzite

Microbial mat colonization of siliciclastic sediment surfaces is common in modern environments (Gerdes *et al.*, 2000; Schieber, 2004) but documented stromatolite occurrences in terrigenous clastic sequences are sparse (Braga & Martín, 2000; Noffke *et al.*, 2003; Draganits & Noffke, 2004). Due to the comparatively high porosity of sandstone that may experience significant reduction during burial compaction (Paxton *et al.*, 2002), early cementation and lithification is essential for preserving domal stromatolites like those from the Eureka Quartzite. The presence of reworked stromatolite fragments along bedding planes of cross-beds (Fig. 6B) and relics of dolomite cement within microbial laminae (Fig. 7E) suggest early cementation/lithification of microbial mats. Enrichment of iron minerals such as pyrite and hematite in dark microbial laminae of the stromatolites (Fig. 7) suggests that microbial mat mineralization may have facilitated early cementation of sand grains by increasing carbonate alkalinity in pore spaces. The increase in alkalinity required to produce early lithification in siliciclastic environments may have to be greater than that in equivalent carbonate environments. Furthermore, carbonate cements in sandstones could easily have been replaced by silica during diagenesis and iron minerals, such as pyrite and hematite, may be the only remaining evidence for the existence of microbial mats in silicified sandstones (Noffke *et al.*, 2006; Schieber, 2007).

Amalgamated or massive intervals within some stromatolites (Fig. 8) provide further insight into the preservation potential of siliciclastic microbial laminae and stromatolites in general within the rock record. Massive intervals (Fig. 8C) contain disseminated iron minerals and, less commonly, detrital clay within intergranular spaces, suggesting the existence of former microbial mineralization. In these stromatolites, however, only the thicker dark laminae (Fig. 8B) reflect the morphological shape of stromatolites. In the absence of these dark laminae, stromatolite identification would be speculative (Schieber, 2007). Massive internal intervals within the stromatolites may have formed either as thin microbial laminae that became amalgamated during compaction and diagenesis or by microbial mats that were less

effective in creating conditions favourable for anaerobic mineralization of organic matter (instead allowing either oxidation or removal by migrating formation water during burial). In either case, stromatolite or microbial laminae may be poorly preserved or difficult to identify. In this regard, thicker microbial mats and/or appropriate microbial ecosystems that promote microbial mat mineralization may be crucial for the preservation of siliciclastic stromatolites.

If anaerobic microbial mat mineralization is important for stromatolite/microbialite preservation, it may have implications for the secular change of stromatolite/microbialite abundance in the rock record. With lower oxygen levels during pre-Phanerozoic times (Holland, 2006), it is conceivable that microbial ecosystems may have promoted anaerobic mat mineralization and preservation. Rising oxygen levels at the end of the Proterozoic (Canfield *et al.*, 2007) may have limited anaerobic mat mineralization to thicker microbial mats or particular microbial mat ecosystems, leading to less-abundant stromatolites/microbialites preserved in the rock record (Fischer, 1965).

CONCLUSIONS

Large domal stromatolites with up to 1·5 m synoptic relief and steep flanks (>45°) are found within the Late Ordovician Eureka Quartzite. These stromatolites appear as either isolated forms or patchy clusters and consist volumetrically of >70% quartz sand; they are found in high-energy siliciclastic environments seemingly hostile to microbial colonization. Microbial mat growth in the Eureka Quartzite may be controlled by the following factors: (i) localized shelter such as sand bars and dunes in upper shoreface and back-barrier tidal flat environments that allowed for the initial colonization of microbial mat-builders; (ii) translucent quartz sand permitted light penetration into the sediment and allowed filamentous cyanobacteria to grow below the sediment surface; (iii) quiescent periods of low sediment flux in upper shoreface and back-barrier tidal flat environments allowed microbial mats to escape burial and repeatedly re-establish after storm events or high tidal events; (iv) biostabilization in established microbial mats prevented further mat removal during erosion, and baffling, trapping and binding of medium-grained to fine-grained sands by filamentous cyanobacteria accelerated accretion of thicker microbial laminae; and (v) localized mat buildups themselves served as nuclei for the establishment of decimetre-scale to metre-scale stromatolites, which subsequently provided shelter or nucleation centres for further microbial colonization, forming patchy stromatolite clusters.

Early cementation was crucial for the preservation of microbial laminae and stromatolites in the Eureka Quartzite. Enrichment of iron minerals such as pyrite and hematite (oxidized from pyrite) in dark microbial laminae within the stromatolites suggests that anaerobic mat mineralization may have facilitated early cementation of sand grains and, thus, the preservation of the stromatolites. Because microbial mats may vary in thickness and in their ecosystems, only thicker microbial mat layers or optimal microbial ecosystems that promote anaerobic mineralization of mat generated organic matter may be preserved in the rock record. In this regard, microbial mats and stromatolites in siliciclastic rocks may have been more abundant than the rock record suggests.

ACKNOWLEDGEMENTS

The research is supported by the Donors of the Petroleum Research Fund administered by the American Chemical Society (PRF 43382-G8 to GJ) and the Bernada French UNLV Geoscience grant (PD). We thank Professors Brian Pratt, Steve Dworkin and Hank Chafetz for their thoughtful comments on earlier versions of this manuscript. We express our sincere appreciation to Professors Daniel Ariztegui (Associate Editor), Brian Pratt and Nora Noffke (journal reviewers) for their careful and constructive criticisms that significantly improved this paper.

REFERENCES

Arp, G., Reimer, A. and **Reitner, J.** (2001) Photosynthesis-induced biofilm calcification and calcium concentrations in Phanerozoic oceans. *Science*, **292,** 1701–1704.

Bartley, J.K., Knoll, A.H., Grotzinger, J.P. and **Sergeev, V.N.** (2000) Lithification and fabric genesis in precipitated stromatolites and associated peritidal carbonates, Mesoproterozoic Billyakah Group, Siberia. *SEPM Spec. Publ.*, **67,** 59–73.

Bertrand-Sarfati, J. (1994) Siliciclastic-carbonate stromatolite domes, in the Early Carboniferous of the Ajers basin (eastern Sahara, Algeria). In: *Phanerozoic Stromatolites III* (Eds J. Bertrand-Sarfati and C. Monty), pp. 395–419. Kluwer Academic, Amsterdam.

Braga, J.C. and **Martín, J.M.** (2000) Subaqueous siliciclastic stromatolites: a case history from late Miocene beach deposits in the Sorbas basin of SE Spain. In: *Microbial*

Sediments (Eds R.E. Riding and S.M. Awramik), pp. 226–232. Springer, Berlin.

Braga, J.C., Martín, J.M. and **Riding, R.** (1995) Controls on microbial dome fabric development along a carbonate-siliciclastic shelf-basin transect, Miocene, SE Spain. *Palaios*, **10,** 347–361.

Burchfiel, B.C., Cowan, D.S. and **Davis, G.A.** (1992) Tectonic overview of the Cordilleran orogen in the western United States. In: *The Cordilleran Orogen: Conterminous U.S.* (Eds B.C. Burchfiel, P.W. Lipman and M.L. Zoback), *Geol. North Am.*, **G-3,** 407–479.

Canfield, D.E., Poulton, S.W. and **Narbonne, G.M.** (2007) Late-Neoproterozoic deep-ocean oxygenation and the rise of animal life. *Science*, **315,** 92–95.

Chafetz, H.S. and **Buczynski, C.** (1992) Bacterially induced lithification of microbial mats. *Palaios*, **7,** 277–293.

Cooper, J.D. and **Keller, M.** (2001) Paleokarst in the Ordovician of the southern Great Basin, USA: implications for sea-level history. *Sedimentology*, **48,** 855–873.

Davis, R.A., Jr (1968) Algal stromatolites composed of quartz sandstone. *J. Sed. Petrol.*, **38,** 953–955.

Draganits, E. and **Noffke, N.** (2004) Siliciclastic stromatolites and other microbially induced sedimentary structures in an early Devonian barrier-island environment (Muth Formation, NW Himalayas). *J. Sed. Res.*, **74,** 191–202.

Fischer, A.G. (1965) Fossils, early life, and atmospheric history. *Natl Acad. Sci. Proc.*, **53,** 1205–1215.

Garlick, W.G. (1988) Algal mats, load structures, and synsedimentary sulfides in Revett Quartzites of Montana and Idaho. *Econ. Geol.*, **32,** 1259–1278.

Gaynor, G.C. and **Swift, D.J.P.** (1988) Shannon sandstone depositional model; sand ridge dynamics on the Campanian western interior shelf. *J. Sed. Res.*, **58,** 868–880.

Gehrels, G.E., Dickinson, W.R., Ross, G.M., Stewart, J.H. and **Howell, D.G.** (1995) Detrital zircon reference for Cambrian to Triassic miogeoclinal strata of western North America. *Geology*, **23,** 831–834.

Gerdes, G. and **Krumbein, W.E.** (1987) Biolaminated deposits. In: *Lecture Notes in Earth Sciences* (Eds S. Bhattacharji, G.M. Friedman, H.J. Neugebauer and A. Seilacher), 183 pp. Springer-Verlag, New York.

Gerdes, G., Krumbein, W.E. and **Reineck, H.-E.** (1985) The depositional record of sandy, versicolored tidal flats (Mellum Island, southern North Sea). *J. Sed. Res.*, **55,** 265–278.

Gerdes, G., Klenke, T. and **Noffke, N.** (2000) Microbial signatures in peritidal siliciclastic sediments: a catalogue. *Sedimentology*, **47,** 279–308.

Grotzinger, J.P. and **Knoll, A.H.** (1999) Stromatolites in Precambrian carbonates: evolutionary mileposts or environmental dipsticks? *Annu. Rev. Earth Planet. Sci.*, **27,** 313–358.

Harris, A.G., Bergstroem, S.M., Ethington, R.L. and **Ross, R.J., Jr** (1979) Aspects of Middle and Upper Ordovician conodont biostratigraphy of carbonate facies in Nevada and southeast California and comparison with some Appalachian successions. *Geol. Stud.*, **26,** 7–44.

Holland, H.D. (2006) The oxygenation of the atmosphere and oceans. *Phil. Trans. Roy. Soc. London, B*, **361,** 903–915.

Kah, L.C. and **Riding, R.** (2007) Mesoproterozoic carbon dioxide levels inferred from calcified cyanobacteria. *Geology*, **35,** 799–802.

Ketner, K.B. (1968) Origin of Ordovician quartzite in the Cordilleran miogeosyncline. *US Geol. Surv. Prof. Pap.* **600-B,** 169–177.

Ketner, K.B. (1986) Eureka Quartzite in Mexico? Tectonic implications. *Geology*, **14,** 1027–1030.

Klein, G. (1975) Tidalites in the Eureka Quartzite (Ordovician) eastern California and Nevada. In: *Tidal Deposits* (Ed. R.N. Ginsberg), pp. 145–151. Springer-Verlag, New York.

Knoll, A.H. and **Semikhatov, M.A.** (1998) The genesis and time distribution of two distinctive Proterozoic stromatolite microstructures. *Palaios*, **13,** 408–422.

Langenheim, R.J. Jr and **Horn, B.** (1978) Algal stromatolites(?) in Eureka Quartzite, southeastern Nevada. *AAPG Annu. Meet. Abstr. Programs*, **62,** 535.

Lee, S.-J., Browne, K.M. and **Golubic, S.** (2000) On stromatolite lamination. In: *Microbial Sediments* (Eds R.E. Riding and S.M. Awramik), pp. 16–24. Springer, Berlin.

Logan, B.W., Rezak, R. and **Ginsburg, R.N.** (1964) Classification and environmental significance of algal stromatolites. *J. Geol.*, **72,** 68–83.

Ludvigson, G.A., Witzke, B.J., Gonzalez, L.A., Carpenter, S.J., Schneider, C.L. and **Hasiuk, F.** (2004) Late Ordovician (Turinian-Chatfieldian) carbon isotope excursions and their stratigraphic and paleoceanographic significance. *Palaeogeogr. Palaeoclimatol. Palaeoecol.*, **210,** 187–214.

Martín, J.M., Braga, J.C. and **Riding, R.** (1993) Siliciclastic stromatolites and thrombolites, late Miocene, S.E. *Spain. J. Sed. Petrol.*, **63,** 131–139.

Martini, I.P., Cascella, A. and **Rau, A.** (1995) The Manciano Sandstone: a shoreface deposit of Miocene basins of the Northern Apennines, Italy. *Sed. Geol.*, **99,** 37–59.

Miller, M.F. (1975) Probable inorganic *Zoophycos*-like structure from a Lower Paleozoic quartzarenite. *J. Paleontol.*, **49,** 1127–1129.

Miller, M.F. (1977) Middle and upper Ordovician biogenic structures and paleoenvironments, southern Nevada. *J. Sed. Res.*, **47,** 1328–1338.

Noffke, N., Gerdes, G., Klenke, T. and **Krumbein, W.E.** (1997) A microscopic sedimentary succession of graded sand and microbial mats in modern siliciclastic tidal flats. *Sed. Geol.*, **110,** 1–6.

Noffke, N., Gerdes, G., Klenke, T. and **Krumbein, W.E.** (2001) Microbially induced sedimentary structures; a new category in the classification of primary sedimentary structures. *J. Sed. Res.*, **71,** 649–656.

Noffke, N., Knoll, A. and **Grotzinger, J.P.** (2002) Sedimentary controls on the formation and preservation of microbial mats in siliciclastic deposits: a case study from the upper Neoproterozoic Nama Group, Namibia. *Palaios*, **17,** 417–426.

Noffke, N., Gerdes, G. and **Klenke, T.** (2003) Benthic cyanobacteria and their influence on the dynamics of peritidal depositional systems (siliciclastic, evaporative salty and evaporative carbonatic). *Earth-Sci. Rev.*, **62,** 163–176.

Noffke, N., Eriksson, K.A., Hazen, R.M. and **Simpson, E.L.** (2006) A new window into Early Archean life: microbial mats in Earth's oldest siliciclastic tidal deposits (3.2 Ga Moodies Group, South Africa). *Geology*, **34,** 253–256.

Patzkowsky, M.E., Slupik, L.M., Arthur, M.A., Pancost, R.D. and **Freeman, K.H.** (1997) Late Middle Ordovician environmental change and extinction: harbinger of the Late Ordovician or continuation of Cambrian patterns? *Geology*, **25,** 911–914.

Paxton, S.T., Szabo, J.O. and **Ajdukiewicz, J.M.** (2002) Construction of an intergranular volume compaction curve for evaluating and predicting compaction and porosity loss in

rigid-grain sandstone reservoirs. *AAPG Bull.*, **86,** 2045–2065.

Poole, F.G., Stewart, J.H., Palmer, A.R., Sandberg, C.A., Madrid, C.A., Ross, R.J. Jr, Hintze, L.F., Miller, M.M. and **Wrucke, C.T.** (1992) Latest Precambrian to latest Devonian time; development of a continental margin. In: *The Cordilleran Orogen: Conterminous U.S.* (Eds B.C. Burchfiel, P.W. Lipman and M.L. Zoback), *Geol. North Am.*, **G-3,** 9–54.

Porada, H. and **Bouougri, E.H.** (2007) Wrinkle structures – a critical review. *Earth-Sci. Rev.*, **81,** 199–215.

Pratt, B.R. (1979) Early cementation and lithification in intertidal cryptalgal structures, Boca Jewfish, Bonaire, Netherlands Antilles. *J. Sed. Petrol.*, **49,** 379–386.

Pratt, B.R. (1982) Stromatolite decline; a reconsideration. *Geology*, **10,** 512–515.

Pratt, B.R. (1984) Epiphyton and Renalcis; diagenetic microfossils from calcification of coccoid blue-green algae. *J. Sed. Res.*, **54,** 948–971.

Pratt, B.R. (2001) Calcification of cyannobacterial filaments: *Girvanella* and the origin of lower Paleozoic lime mud. *Geology*, **29,** 763–766.

Reineck, H.-E. and **Gerdes, G.** (1997) Tempestites in recent shelf and tidal environments of the southern North Sea. *Courier Forschungsinstitut Senckenberg*, **201,** 361–370.

Riding, R. (2000) Microbial carbonates; the geological record of calcified bacterial-algal mats and biofilms. In: *Millennium Reviews* (Eds J.L. Best, C. Fielding, I. Jarvis and P. Mozley), *Millen. Rev., Sedimentol. Suppl. 1*, **47,** 179–214.

Riding, R. (2006) Cyanobacterial calcification, carbon dioxide concentrating mechanisms, and Proterozoic-Cambrian changes in atmospheric composition. *Geobiology*, **4,** 299–316.

Saltzman, M.R. and **Young, S.A.** (2005) Long-lived glaciation in the Late Ordovician? Isotopic and sequence-stratigraphic evidence from western Laurentia. *Geology*, **33,** 109–113.

Schieber, J. (1998) Possible indicators of microbial mat deposits in shales and sandstones: examples from mid-Proterozoic Belt Supergroup, Montana, USA. *Sed. Geol.*, **120,** 105–124.

Schieber, J. (1999) Microbial mats in terriginous clastics: the challenge of identification in the rock record. *Palaios*, **14,** 3–12.

Schieber, J. (2004) Microbial mats in the siliciclastic rock record: a summary of diagnostic features. In: *The Precambrian Earth: Tempos and Events* (Eds P.G. Eriksson, W. Altermann, D.R. Nelson, W.U. Mueller and O. Catuneanu), *Dev. Precambrian Geol.*, **12,** 663–673. Elsevier, Amsterdam.

Schieber, J. (2007) Oxidation of detrital pyrite as a cause for marcasite formation in marine lag deposits from the Devonian in the eastern US. *Deep-Sea Res. II*, **54,** 1312–1326.

Schieber, J. and **Riciputi, L.** (2004) Pyrite and marcasite coated grains in the Ordovician Winnipeg Formation, Canada: an intertwined record of surface conditions, stratigraphic condensation, geochemical ''reworking'' and microbial activity. *J. Sed. Res.*, **75,** 907–920.

Schwartz, H.E., Einsele, G. and **Herm, D.** (1975) Quartz-sandy, grazing-contoured stromatolites from coastal embayments of Mauritania, West Africa. *Sedimentology*, **22,** 539–561.

Soudry, D. and **Weissbrod, T.** (1995) Morphogenesis and facies relationships of thrombolites and siliciclastic stromatolites in a Cambrian tidal sequence. *Palaeogeogr. Palaeoclimatol. Palaeoecol.*, **114,** 339–355.

Stone, P. and **Stevens, C.H.** (1988) Pennsylvanian and Early Permian paleogeography of east-central California: implications for the shape of the continental margin and the timing of continental truncation. *Geology*, **16,** 330–333.

Sweet, W.C. (2000) Conodonts and biostratigraphy of upper Ordovician strata along a shelf to basin transect in central Nevada. *J. Paleontol.*, **74,** 1148–1160.

Tillman, R.W. and **Martinsen, R.S.** (1984) The Shannon shelf-ridge sandstone complex, Salt Creek anticline area, Powder River Basin, Wyoming. In: *Siliciclastic Shelf Sediments* (Eds R.W. Tillman and C.T. Seimers), *SEPM Spec. Publ.*, **34,** 85–142.

Manuscript received 3 January 2008; revision accepted 13 October 2008